
Application of approximating-functions method to the problems of planar waveguides with non-magnetic media

Zolotariov D.

Independent researcher. Kharkiv, Ukraine;
ORCID: <https://orcid.org/0000-0003-4907-7810> denis@zolotariov.org.ua

Received: 25.01.2022

Abstract. We analyze application of a so-called approximating-functions method, a special case of a known finite-element method with polynomials of Lagrange type of the third order as interpolating functions, to solving electrodynamics problems for planar waveguides in the spatial and time domains with Volterra integral equations. Our main goal is expanding the field of applicability of the approximating-functions method towards three-dimensional problems in the time domain. This should enable solving a much wider range of problems, including those involving material media with non-stationary and nonlinear properties. We also examine whether our approach meets the general convergence criteria imposed by the finite-element method.

Keywords: method of approximating functions, planar waveguides, analytical and numerical methods, nonlinear media.

UDC: 535, 51-73

1. Introduction

Studies of electromagnetic-field propagation in the waveguides with linear or nonlinear materials have a fundamental importance. This is because the corresponding processes are used in optical communications, nanocomputing and some others modern branches of technologies, where electromagnetic-wave interactions with material media take place in time and in confined spatial regions. Modelling these initial-boundary problems requires development of both adequate mathematical models and relevant techniques.

A Volterra integral-equation method represents an approach based on integral equations, which is equivalent to the Maxwell's equations [1, 2]. It is used to solve many electrodynamics problems in 1D to 3D space and time domain. Besides of equivalence to the Maxwell's equations, the method reveals a number of advantages: natural description of non-stationary and nonlinear features, unified definition of the problems inside and outside of homogeneity approximation for material media, and inclusion of both initial and boundary conditions in the same equations. As a consequence, this method simplifies essentially the formulation and solution of many problems associated with both fundamental studies and modelling of real-life tasks.

One should also mention the following important features of this method: the form of the working equations is the Volterra integral equation of the second kind, which remains the same for different media and different laws of parameters' variation. Moreover, it does not depend on the specific feature of initial electromagnetic signal. Then universal modelling algorithms can be applied to a wide range of electrodynamics problems [3]. For example, an approximate solution can be constructed by a standard method of successive approximations or by a direct numerical-integration method [4]. Nonetheless, the combined analytical-numerical approximating-functions method represents a modern approach to building qualitative solutions.

The approximating-functions method is a special case of a known finite-element method, which is based on dividing a domain of the problem using a mesh of cells and constructing a solution as analytical approximation by Lagrange polynomials in each of the cells. The solution of the Volterra integral equation in this case can be reduced to the solution of a system of nonlinear algebraic equations. The latter is solved by a standard Newton's method or any other method suitable for a given problem.

The fundamentals of this method for a general 1D case have been described for the first time in Refs. [5, 6]. It has been extended to the 2D case [7, 8] with the purpose of solving the problems of electrodynamics by the Volterra integral equation method in 1D space and time. To improve its performance and reliability, an approach of building fault-tolerant calculations has been suggested in Ref. [9]. Later on, it has been used to build a microservice computing node in a cloud application [10, 11].

Up to date, the approximating-functions method as a part of the Volterra integral equation method has never been applied to modelling the 3D problems concerned with planar waveguides. On the other hand, such extension of applicability field of this approach would enable solving a much wider range of problems, including those arising for the media with non-stationary properties. These problems are the subject of our study.

2. Problem statement

Let us consider a planar waveguide composed of a non-magnetic medium with losses. Suppose that a signal propagates along a single axis only (z axis, to be specific), with no dependence on the transversal (e.g., y) coordinate. According to the Volterra integral equation method [3], a general equation for this situation acquires the form

$$\mathbf{E} = \mathbf{E}_0 + \frac{1}{4\pi} \left(\nabla \nabla - \frac{1}{v^2} \frac{\partial^2}{\partial t^2} \hat{I} \right) \int_0^\infty dt' \int_{-\infty}^\infty dz' \int_{-\infty}^\infty dx' \frac{2v}{\sqrt{v^2 \Delta t^2 - R_\perp^2}} \times \theta(v^2 \Delta t^2 - R_\perp^2) \chi \left\{ \frac{1}{\varepsilon_0 \varepsilon} \mathbf{P} + v^2 \mu_0 \int_0^{t'} dt'' \mathbf{j} \right\}, \quad (1)$$

where \mathbf{E}_0 denotes the undisturbed electric field and \mathbf{P} the polarization of a medium inside some slab, which has the electromagnetic characteristics different from those of environment outside it, \mathbf{j} is a conductivity current inside the slab, ε the permittivity of medium in the environment, $v = c/\sqrt{\varepsilon}$, μ_0 stands for the vacuum permeability, c the speed of light in vacuum. Here the SI system of units is used. The function χ is equal to unity inside the waveguide and zero outside it, ∇ implies the Hamilton operator, \hat{I} the singular operator, θ the Heaviside step function, (t', x', z') are the integration variables corresponding to (t, x, z) , $R_\perp^2 = (x - x')^2 + (z - z')^2$, and $\Delta t = t - t'$.

As usual for the electromagnetic fields in longitudinally uniform structures, the fields in the waveguide can be expanded into their longitudinal and transverse components:

$$\begin{aligned} E_z(t, x, z) = & E_{0z}(t, x, z) + \frac{1}{4\pi} \left(\partial_{zz}^2 - \frac{1}{v^2} \frac{\partial^2}{\partial t^2} \right) \int_0^\infty dt' \int_{-\infty}^\infty dz' \int_{-\infty}^\infty dx' \frac{2v}{\sqrt{v^2 \Delta t^2 - R_\perp^2}} \\ & \times \theta(v^2 \Delta t^2 - R_\perp^2) \chi \left\{ \frac{1}{\varepsilon_0 \varepsilon} P_z + v^2 \mu_0 \int_0^{t'} dt'' j_z \right\} + \frac{1}{4\pi} \left(\partial_{zx}^2 \right) \int_0^\infty dt' \int_{-\infty}^\infty dz' \int_{-\infty}^\infty dx' \\ & \times \frac{2v}{\sqrt{v^2 \Delta t^2 - R_\perp^2}} \theta(v^2 \Delta t^2 - R_\perp^2) \chi \left\{ \frac{1}{\varepsilon_0 \varepsilon} P_x + v^2 \mu_0 \int_0^{t'} dt'' j_x \right\} \end{aligned} \quad (2)$$

$$\begin{aligned}
 E_x(t, x, z) = & E_{0x}(t, x, z) + \frac{1}{4\pi} \left(\partial_{xx}^2 - \frac{1}{v^2} \frac{\partial^2}{\partial t^2} \right) \int_0^\infty dt' \int_{-\infty}^\infty dz' \int_{-\infty}^\infty dx' \frac{2v}{\sqrt{v^2 \Delta t^2 - R_\perp^2}} \\
 & \times \theta(v^2 \Delta t^2 - R_\perp^2) \chi \left\{ \frac{1}{\varepsilon_0 \varepsilon} P_x + v^2 \mu_0 \int_0^{t'} dt'' j_x \right\} + \frac{1}{4\pi} \left(\partial_{xz}^2 \right) \int_0^\infty dt' \int_{-\infty}^\infty dz' \int_{-\infty}^\infty dx' \\
 & \times \frac{2v}{\sqrt{v^2 \Delta t^2 - R_\perp^2}} \theta(v^2 \Delta t^2 - R_\perp^2) \chi \left\{ \frac{1}{\varepsilon_0 \varepsilon} P_z + v^2 \mu_0 \int_0^{t'} dt'' j_z \right\}
 \end{aligned} \quad (3)$$

Eqs. (2) and (3) describe electromagnetic-field evolution in the time interval $t \in [0, \infty)$. If the observation point (z, x) belongs to a waveguide core, they formulate the problem for the field inside the slab. Outside the core, the expressions are quadrature formulas for calculating the fields in the cladding, taking into account the field in the core.

Let us assume that the x variable in the slab varies within the range $x \in [-b/2, b/2]$, where b is a constant introduced for symmetry purposes only. Then the integration area can be specified by the two conditions:

$$v^2(t-t')^2 - (x-x')^2 - (z-z')^2 > 0 \text{ and } \chi = 1. \quad (4)$$

Fig. 1 presents this area for some point (t, x, z) . As the equation of each circle at the base of the cones is $(x-x')^2 + (z-z')^2 = v^2(t-t')^2$, the appropriate moments can be represented through it as $v|t-t'| = b/2 - x$ and $v|t-t'| = b/2 + x$.

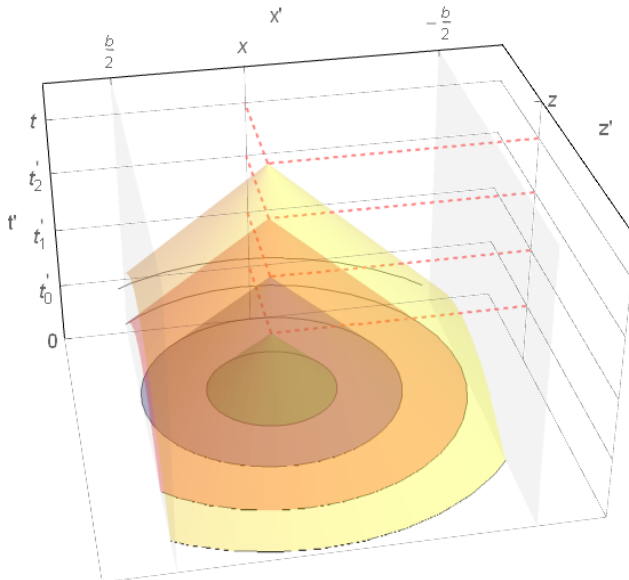


Fig. 1. Cones of integration in a slab.

For the time moment t'_0 , the base of the cone fits completely into the area from Eq. (4) and the integration can be performed as if there were no boundaries for x at all. After the time moment $t'_1 = t - (b/2 - x)/v$, when the base of the cone from Eq. (4) touches the waveguide wall $x' = b/2$, its influence must be included. After the time moment $t'_2 = t - (b/2 + x)/v$, when it also touches the second wall $x' = -b/2$, the contributions of both walls arise.

Therefore there is no influence of the waveguide walls in the interval $[0, t'_1]$ (see green and red cones in Fig. 1). The influence of only one wall must be taken into account in the interval $(t'_1, t'_2]$ (an orange cone in Fig. 1), and the influence of both walls is considered in the interval $(t'_2, t]$ (a yellow cone in Fig. 1).

3. Approximating functions

Similarly to Ref. [3], we construct a mesh of semi-closed cuboids in the space-time cuboid D while solving the Volterra integral equation in the 2D space and time area (t, x, z) :

$$D = \cup D_{ijk},$$

$$D_{ijk} = \{ih \leq t < (i+1)h, \quad jh \leq x < (j+1)h, \quad kh \leq z < (k+1)h\}, \quad (5)$$

$$i = \overline{0, n-1}, \quad j = \overline{0, m-1}, \quad k = \overline{0, p-1}$$

where h is the length of cuboid edge, i.e. a mesh of spacing.

The solution of the equation can be approximately constructed as a sum of piecewise-smooth functions $\hat{E}_{i,j,k}(t, x, z)$, each of which is determined in the corresponding grid cell D_{ijk} :

$$E(t, x, z) \approx \hat{E}(t, x, z) = \sum_{i=0}^{n-1} \sum_{j=0}^{m-1} \sum_{k=0}^{p-1} \hat{E}_{i,j,k}(t, x, z). \quad (6)$$

These functions are constructed from the eight approximating polynomials T with the corresponding weighting coefficients $c_{i,j,k}$:

$$\hat{E}_{i,j,k}(t, x, z) = \sum_{d_1=0}^1 \sum_{d_2=0}^1 \sum_{d_3=0}^1 c_{i+d_1, j+d_2, k+d_3} \cdot T_{i,j,k}^{d_1, d_2, d_3}(t, x, z). \quad (7)$$

Here the approximating (interpolating) polynomials are presented in the form of Lagrange polynomials of the third order at each coordinate point. In general, they can be written as

$$T_{i,j,k}^{d_1, d_2, d_3}(t, x, z) = [T_i^{d_1}(t)]^3 \cdot [T_j^{d_2}(x)]^3 \cdot [T_k^{d_3}(z)]^3, \quad (8)$$

$$T_i^d(s) = (1-d) + (-1)^{d+1} \frac{s-ih}{h}, \quad d = \overline{0, 1}, \quad (9)$$

where s is some variable. These functions satisfy the requirements [12] for the basic functions of the finite-element method: they are dimensionless and mutually orthogonal, continuous within the cell where they are defined, and their total sum at any vertex of this cell is equal to unity.

Being defined in the corresponding cuboids, the functions are mutually orthogonal and have equal norms in the whole range where the problem is defined:

$$\int_{0-b/2}^{T} \int_{-b/2}^{b/2} \int_{-\infty}^{\infty} T_{i,j,k}^{d_1, d_2, d_3}(t, x, z) T_{p,q,l}^{d_4, d_5, d_6}(t, x, z) dz dx dt$$

$$= \int_{ih}^{(i+1)h} [T_i^{d_1}(t)]^3 [T_p^{d_4}(t)]^3 dt \cdot \int_{jh}^{(j+1)h} [T_j^{d_2}(x)]^3 [T_q^{d_5}(x)]^3 dx \quad (10)$$

$$\times \int_{kh}^{(k+1)h} [T_k^{d_3}(z)]^3 [T_l^{d_6}(z)]^3 dz = (h/7)^3 \delta_{ip} \delta_{jq} \delta_{kl},$$

where δ_{ip} is the Kronecker symbol and T the constant (the time limit of integration). When we

have $i = p$, $j = q$ and $k = l$, the integrals take the values of the norm, which equals to $(h/7)^3$. In the alternative cases, the functions under the integrals are products of two incompatible functions with different regions of definition, which gives a zero value of the integral.

The sum of the polynomials taken at any vertex of the mesh cell (i, j, k) is equal to unity. As an example, this can be easily demonstrated for the point (ih, jh, kh) :

$$\sum_{d_1=0}^1 \sum_{d_2=0}^1 \sum_{d_3=0}^1 T_{i,j,k}^{d_1,d_2,d_3}(t,x,z) \Big|_{(ih,jh,kh)} = [T_i^0(ih)]^3 \cdot [T_j^0(jh)]^3 \cdot [T_k^0(kh)]^3 = 1. \quad (11)$$

The calculations are essentially the same at the point $((i+1)h, jh, kh)$, with the only difference that we have $T_j^0((j+1)h) = 0$ and $T_j^1((j+1)h) = 1$. The relevant proofs for the coordinates x and z is also the same.

For the convergence of the method in the case of approximating polynomials given by Eq. (8), it is necessary that the approximated functions $\hat{E}_{i,j,k}(t,x,z)$ be specified in the form of polynomial of at least degree two and be continuous in between and within the mesh cells.

Now let us show that $\hat{E}_{i,j,k}(t,x,z)$ is continuous on the boundaries of the cells along the coordinate x for the two adjacent cells (i, j, k) and $(i, j+1, k)$:

$$\begin{aligned} \hat{E}_{i,j,k}(t, (j+1)h, z) &= \sum_{d_1=0}^1 \sum_{d_3=0}^1 c_{i+d_1, j+1, k+d_3} \cdot [T_i^{d_1}(t)]^3 \cdot [T_k^{d_3}(z)]^3, \\ \hat{E}_{i, j+1, k}(t, (j+1)h, z) &= \sum_{d_1=0}^1 \sum_{d_3=0}^1 c_{i+d_1, j+1, k+d_3} \cdot [T_i^{d_1}(t)]^3 \cdot [T_k^{d_3}(z)]^3. \end{aligned} \quad (12)$$

Taking into account that the functions given by Eq. (8) are symmetric with respect to the change of variables, one can easily prove that the approximated functions $\hat{E}_{i,j,k}(t,x,z)$ are continuous on the remaining borders of the cells.

The properties of derivatives of the approximated functions are worth noting. The modules of the first derivatives and the second mixed derivatives are continuous in between the cells. Let us prove this for the case of x coordinate:

$$\frac{\partial \hat{E}_{i,j,k}(t,x,z)}{\partial x} \Big|_{x=(j+1)h} = \frac{3}{h} \sum_{d_1=0}^1 \sum_{d_3=0}^1 c_{i+d_1, j+1, k+d_3} \cdot [T_i^{d_1}(t)]^3 \cdot [T_k^{d_3}(z)]^3, \quad (13)$$

$$\frac{\partial \hat{E}_{i, j+1, k}(t,x,z)}{\partial x} \Big|_{x=(j+1)h} = -\frac{3}{h} \sum_{d_1=0}^1 \sum_{d_3=0}^1 c_{i+d_1, j+1, k+d_3} \cdot [T_i^{d_1}(t)]^3 \cdot [T_k^{d_3}(z)]^3,$$

$$\frac{\partial^2 \hat{E}_{i,j,k}(t,x,z)}{\partial x \partial z} \Big|_{x=(j+1)h} = \frac{9}{h^2} \sum_{d_1=0}^1 \sum_{d_3=0}^1 c_{i+d_1, j+1, k+d_3} \cdot [T_i^{d_1}(t)]^3 \cdot [T_k^{d_3}(z)]^2 \cdot (-1)^{d_3+1}, \quad (14)$$

$$\frac{\partial^2 \hat{E}_{i, j+1, k}(t,x,z)}{\partial x \partial z} \Big|_{x=(j+1)h} = -\frac{9}{h^2} \sum_{d_1=0}^1 \sum_{d_3=0}^1 c_{i+d_1, j+1, k+d_3} \cdot [T_i^{d_1}(t)]^3 \cdot [T_k^{d_3}(z)]^2 \cdot (-1)^{d_3+1}.$$

Note that the proof remains the same for the t and z coordinates.

The second derivatives are also continuous in between the cells:

$$\left. \frac{\partial^2 \hat{E}_{i,j,k}(t,x,z)}{\partial^2 x} \right|_{x=(j+1)h} = \frac{6}{h^2} \sum_{d_1=0}^1 \sum_{d_3=0}^1 c_{i+d_1,j+1,k+d_3} \cdot [T_i^{d_1}(t)]^3 \cdot [T_k^{d_3}(z)]^3. \quad (15)$$

$$\left. \frac{\partial^2 \hat{E}_{i,j+1,k}(t,x,z)}{\partial^2 x} \right|_{x=(j+1)h} = \frac{6}{h^2} \sum_{d_1=0}^1 \sum_{d_3=0}^1 c_{i+d_1,j+1,k+d_3} \cdot [T_i^{d_1}(t)]^3 \cdot [T_k^{d_3}(z)]^3.$$

Finally, the derivatives coincide with each other at the cell boundaries. Due to the symmetry of Eq. (8) with respect to the change of variables, this dependence is also preserved for the derivatives with respect to t and z .

The important advantage of these polynomials is that they are defined as a product of polynomials, each of which depends only on single variable. This implies relatively easy calculations of integrals and derivatives.

Since the sum of all polynomials is equal to unity at any vertex of any cell, the coefficients $c_{i,j,k}$ represent in fact the approximate values of the function \hat{E} at the vertex (i, j, k) :

$$c_{i,j,k} = \hat{E}(t_i, x_j, z_k) = \hat{E}(ih, jh, kh). \quad (16)$$

So, the approximate relations for the longitudinal (E_z) and transverse (E_x) field components obtained from Eqs. (2) and (3) have the following forms:

$$\hat{E}_z(t, x, z) = \sum_{i=0}^{n-1} \sum_{j=0}^{m-1} \sum_{k=0}^{p-1} \sum_{d_1=0}^1 \sum_{d_2=0}^1 \sum_{d_3=0}^1 v_{i+d_1,j+d_2,k+d_3} \cdot T_{i,j,k}^{d_1,d_2,d_3}(t, x, z), \quad (17)$$

$$\hat{E}_x(t, x, z) = \sum_{i=0}^{n-1} \sum_{j=0}^{m-1} \sum_{k=0}^{p-1} \sum_{d_1=0}^1 \sum_{d_2=0}^1 \sum_{d_3=0}^1 c_{i+d_1,j+d_2,k+d_3} \cdot T_{i,j,k}^{d_1,d_2,d_3}(t, x, z). \quad (18)$$

Substitution of Eq. (17) into Eq. (2) and calculation of the resulting function at the points (t_i, x_j, z_k) ($i = \overline{0, n}, j = \overline{0, m}, k = \overline{0, p}$) gives a system of nonlinear algebraic equations for the weighting coefficients $c_{i,j,k}$, which can be solved by the Newton's method. The problem for Eq. (3) is solved in a similar manner, with substitution Eq. (18).

4. Algorithm for approximation of the cone

As mentioned above, the area of integration in Eqs. (2) and (3) for the region inside the waveguide is bounded in the x coordinate by a cone determined by the inequality given by Eq. (4). The approximation for this cone can be constructed basing on this inequality and taking discrete cell coordinates $(t'_i = ih, x'_j = jh, z'_k = kh)$.

An example of how to build this approximation for some point (t, x, z) is illustrated in Fig. 2. Here, the time moment t has to be far enough from $t' = 0$ for the cone to intersect with the both planes that bound the waveguide along the x coordinate: $t_{\min}^{b/2}$ is determined by the intersection with the plane $x = -b/2$ and $t_{\min}^{b/2}$ by the intersection with the plane $x = b/2$.

For clarity, Fig. 2 shows only the approximation of the outer surface of the cone, without its inner part, which also constrains the cone along the z axis. Fig. 2 also displays the original cone as a semitransparent red surface that extends beyond the x axis of the waveguide. The latter is shown to demonstrate the constraints introduced by the waveguide.

After constructing approximation of the cone, the result is filtered. The filtration is needed to remove the situations when the result depends on the approximation step or some other parameter.

Then the cone approximation for the levels (or the ‘circles’) t_i and t_{i+1} includes the cells with the same coordinates (x, z) lying on the cone surface (i.e., the cuboids located farthest from the centre of the cone on a single layer). To simplify the process of solving the problem, these situations should be excluded.

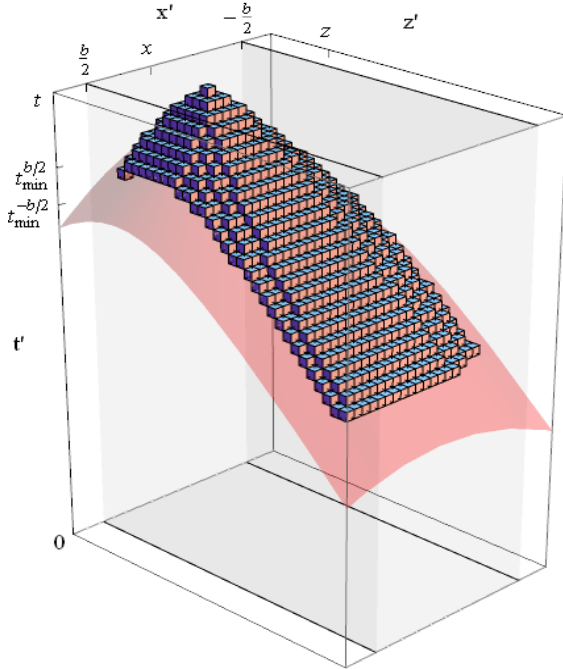


Fig. 2. Approximation of integration cone by cuboid cells, as performed in the case of integration point (t, x, z) in a slab.

The filtering algorithm is simple. If the approximating cuboid is located on the surface of the cone in the layer t_{i-1} , it must be excluded from the layer t_i . After that, all the levels will include no common approximation cuboids on the cone surface.

An example of this approximation of the cone (after filtering at some point (t, x, z)) is shown by a level line graph in Fig. 3. Here the level lines for the original cone (black concentric circles in Fig. 3) are also shown. For a convenience, each of the level lines is presented by the same colour. Namely, the orange colour marks the top of the cone and the yellow one its base.

5. Conclusions

In this work, we present how to extend the approximating-functions method in order to solve the electrodynamics problems that arise for the planar waveguides in the 2D space the time domains, using the Volterra integral equation method. It is demonstrated that the above problem can be divided into two subproblems for the longitudinal and transverse coordinates bounding the waveguide. Each subproblem can be reduced to solving the integral Volterra equation of the second kind.

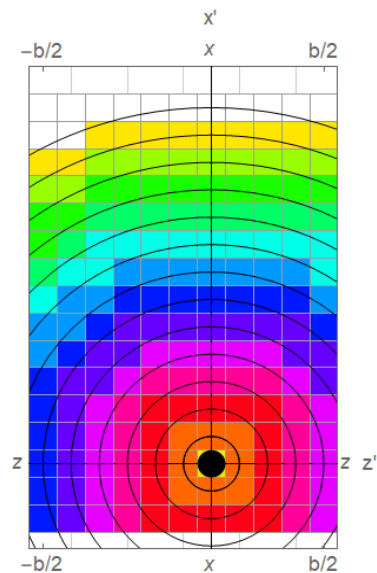


Fig. 3. Level lines for the cone approximation obtained after filtration, and the corresponding circles (layers) of the original cone.

The domain of integration for each of the equations is given by a cone, which can be approximated by cuboids. Then the approximating-functions method can be applied. We also present the algorithms needed for constructing the approximation of this cone by the cuboids and for filtering the obtained approximation, in order to eliminate complex and ambiguous situations that can appear in the process of solving the problem.

The approximating polynomials chosen as interpolation functions in each cuboid are the Lagrange-type polynomials of the third order at each coordinate. We have shown that these polynomials satisfy all the requirements for the basic functions imposed by the finite-element method and, hence, the associated approximating-functions method. As a consequence, we have demonstrated that the polynomials suggested by us satisfy the convergence criteria required by the finite-element method. The relationship between the first and second derivatives defined at the boundaries of the cuboids is also derived.

Since the approximating-functions method is a special case of the finite-element method, the real accuracy of the obtained solution depends on discretization of the domain where the problem is defined: i.e., the more elements, the higher the accuracy of the solution.

Acknowledgments

The author thanks A. Nerukh for his timely help and recommendations during preparation of this manuscript.

References

1. Shifman Y and Leviatan Y, 2001. On the use of spatio-temporal multiresolution analysis in method of moments solutions of transient electromagnetic scattering. *IEEE Trans. Anten. Propag.* **49**: 1123–1129.
2. Gomez M R, Salinas A and Bretones A R, 1992. Time-domain integral equation methods for transient analysis. *IEEE Anten. Propag. Mag.* **34**: 15–24.
3. Nerukh A and Benson T. *Non-stationary electromagnetics: An integral equations approach*. Singapore: Jenny Stanford Publishing, 2018.
4. Nédélec J C. *Acoustic and electromagnetic equations: integral representations for harmonic problems*. New York: Springer, 2001.
5. Anish D, Dasgupta A and Sarkar G, 2006. A new set of orthogonal functions and its application to the analysis of dynamic systems. *J. Franklin Inst.* **343**: 1–26.
6. Maleknejad K, Almasieh H and Roodaki M, 2010. Triangular functions (TF) method for the solution of nonlinear Volterra–Fredholm integral equations. *Commun. Nonlin. Sci. Numer. Simulat.* **10**: 10–12.
7. Zolotariov D and Nerukh A, 2011. Extension of the approximation functions method for 2D non-linear Volterra integral equations. *Appl. Radioelectron.* **10**: 39–44.
8. Nerukh A, Zolotariov D and Benson T, 2015. The approximating functions method for nonlinear Volterra integral equations. *Opt. Quant. Electron.* **47**: 2565–2575.
9. Zolotariov D, 2021. The new modification of the approximating functions method for cloud computing. *Intern. J. Math. Comp. Res.* **9**: 2376–2380.
10. Zolotariov D, 2020. The distributed system of automated computing based on cloud infrastructure. *Innov. Techn. Sci. Sol. Ind.* **14**: 47–55.
11. Zolotariov D, 2021. Microservice architecture for building high-availability distributed automated computing system in a cloud infrastructure. *Innov. Techn. Sci. Sol. Ind.* **17**: 13–22.
12. Romyantsev A V. *Finite element method in heat conduction problems*. Moscow: Russian State University, 2010.

Zolotariov D. 2022. Application of approximating-functions method to the problems of planar waveguides with non-magnetic media Ukr.J.Phys.Opt. **23**: 15 – 23.

doi: 10.3116/16091833/23/1/15/2022

***Анотація.** У статті представлено використання методу апроксимуючих функцій - особливого випадку методу скінченних елементів з поліномами типу Лагранжа третього порядку у якості інтерполюючих функцій, для розв'язання задач електродинаміки в плоскому хвилеводі в просторовій та часовій області з використанням інтеграла Вольтерра. Основна мета цієї роботи – розширити область застосування методу апроксимуючих функцій до тривимірних задач у часовій області, що дозволить вирішувати набагато ширший спектр задач, у тому числі задачі із середовищами з нестационарними та нелінійними властивостями. Запропонований метод перевірено на відповідність критеріям збіжності, встановленим методом скінченних елементів.*